Research article: Single Channel Electrocardiography Optimizes the Diagnostic Accuracy of Bicycle Ergometry

Running tittle: Recent advances in IHD diagnosis

Authors' list: Basheer Abdullah Marzoog[1,*], Magomed Abdullaev[1], Alexander Suvorov[1], Peter Chomakhidze[1], Daria Gognieva[1], Nina Vladimirovna Gagarina[2], Natalia Mozzhukhina[3], Sergey Vladimirovich Kostin[4], Afina Aftandilovna Bestavashvili[1], Ekaterina Fominykha[2], Philipp Kopylov[1]

[1] World-Class Research Center «Digital Biodesign and Personalized Healthcare», I.M. Sechenov First Moscow State Medical University (Sechenov University), 119991 Moscow, Russia; postal address: Russia, Moscow, 8-2 Trubetskaya street, 119991.

[2] University clinical Hospital number 1, Radiology department, I.M. Sechenov First Moscow State Medical University (Sechenov University), 119991 Moscow, Russia; postal address: Russia, Moscow, 8-2 Trubetskaya street, 119991.

[3] University clinical Hospital number 1, Health Management Clinic, I.M. Sechenov First Moscow State Medical University (Sechenov University), 119991 Moscow, Russia; postal address: Russia, Moscow, 8-2 Trubetskaya street, 119991.

[4] National Research Ogarev Mordovia State University. Russia. Republic of Mordovia. Saransk. Bolshevistskaya str. 68, Saransk. Mordovia Republic. 430005.

[*]Corresponding author: Basheer Abdullah Marzoog, M.D., Ph.D. cardiology student at Sechenov First Moscow State Medical University at the World-Class Research Center "Digital biodesign and personalized healthcare". (marzug@mail.ru, +79969602820). Address: Russia, Moscow, 8-2 Trubetskaya street, 119991. Postal address: Russia, Moscow, 8-2 Trubetskaya street, 119991. ORCID: 0000-0001-5507-2413, Scopus ID: 57486338800

Competing interests: No competing interests regarding the publication.

"Posted history: This manuscript was previously posted to MedRxiv: doi: https://doi.org/10.1101/2024.04.20.24306122"

Abstract

Background: Ischemic heart disease (IHD) has the highest mortality rate in the globe. This returns to the poor diagnostic and therapeutic strategies including the early prevention methods.

Aims: To assess the changes in the single channel electrocardiography (SCECG) at rest and on exercise test in patients with vs without IHD confirmed by stress computed tomography myocardial perfusion (CTP) imaging with vasodilatation stress-test.

Objectives: IHD frequently have preventable risk factors and causes that lead to the disease appearance. However, the lack of the proper diagnostic and prevention tools remains a global challenge in or era despite the current scientific advances.

Material and methods: A single center observational study included 38 participants from Moscow. The participants aged ≥ 40 years and given a written consent to participate in the study. Both groups, G1=19 with vs G2=19 without post stress induced myocardial perfusion defect, passed consultation by cardiologist, anthropometric measurements, blood pressure and pulse rate, echocardiography, cardio-ankle vascular index, performing bicycle ergometry, recording 3-minutes SCECG (using CARDO-QVARK) before and just after bicycle ergometry, and then performing CTP. The LASSO regression with nested cross-validation was used to find association between CARDO-QVARK parameters and the existence of the perfusion defect. Statistical processing carried out using the R programming language v4.2 and Python v.3.10 [^R].

Results: The CARDO-QVARK parameters analysis have a specificity 63.2 % [95 % confidence interval (CI); 0.391 ; 0.833], sensitivity 73.7 % [95 % CI ; 0.533 ; 0.929], area under the curve (AUC) 68.4 % [95 % CI ; 0.527 ; 0.817] in compare to bicycle ergometry (AUC; 55.3 %), based on our study results.

Conclusion: The SCECG have significantly higher diagnostic accuracy in compare to bicycle ergometry. CARDO-QVARK has the potential to improve the diagnostic accuracy of the bicycle ergometry.

Other: Further investigations required to uncover the hidden capabilities of CARDO-QVARK in the diagnosis of ischemic heart disease.

Keywords: IHD, Single channel electrocardiography, CTP, Prevention, Risk Factors, Stress Test, Machine Learning Model

Introduction

Ischemic heart disease remains the leading challenge in terms of mortality and morbidity despite the advances in the used methods for diagnosis and prevention. However, the early prevention in terms of evaluation of the ischemic heart disease in early period still underestimated. The current attention of the scientists paid to the prevention rather than diagnosis and treatment. In this manner, the scientific community developed several cost-effective methods to be confirmed for clinical use for early prevention of ischemic heart disease, including the use of the single channel electrocardiography and exhaled breath analysis in coronary heart disease prevention [1].

Ischemic heart diagnosis using single channel electrocardiography (ECG) remains in the development stage and require further elaboration in the context of the sensitivity and specificity. Several kinds of single channel ECG has been used in the clinical trials including CARDO-QVARK , Apple Watch, Kardia, Zio, BioHarness, Bittium Faros and Carnation Ambulatory Monitor [1–8]. Single channel ECG has been used to diagnosis myocardial infarction and monitoring patients with chronic heart disease and heart failure as well as to classify heartbeat [9–11].

Currently there are several kinds of single channel ECG used for commercial purposes and clinical trials. The accuracy and quality of these single channel ECGs various. The uses of single channel ECGs are various including distant monitoring of patients with arrythmias, as a Holter monitoring, and for monitoring for chronic heart failure [12, 13, 22, 14–21]. The currently available single channel ECGs in the market include Apple Watch, Kardia, Zio, Cardiostat, BioHarness, Bittium Faros and Carnation Ambulatory Monitor [13, 23].

Single-channel ECG has key features that can aid in diagnosing ischemic heart disease include detecting ischemia through ECG alterations, hemodynamic changes, and clinical signs and symptoms [24]. Additionally, vectorcardiography, a technique that records cardiac electrical activity as closed loops, can be useful for training in electrocardiography and detecting cardiac ischemia [24, 25]. Portable and fast electrode placement devices allow for good-quality ECG tracings, making single-channel ECG accessible and efficient [24].

In comparison of single-channel ECG to multi-channel ECG in detecting ischemic heart disease shows that modern ECG systems with vector-based electrocardiography can improve the detection of ECG alterations typical for ischemia compared to the conventional 12-lead ECG [26]. Single-channel consumer ECG devices, such as smartwatches, can be useful for detecting and monitoring arrhythmias but have limitations in detecting ST-segment deviations indicating myocardial infarction or ischemic episodes [27].

The usage of single channel in ischemic heart disease has not been previously investigated and requires further elucidation.

Material and methods

A cohort, prospective single center cohort study included 38 participants. According to the results of the CTP, the participates divided in to two groups. The first group participants without stress induced myocardial perfusion defect and the second group with stress induced myocardial perfusion defect on the CTP. The participants are randomly chosen. A written consent has been taken from the participants. The study registered on clinicaltrials.gov (NCT06181799), and the study approved by the ethical commitment of the Sechenov University, Russia, from "Ethics Committee Requirement № 19-23 from 26.10.2023".

The study evaluated continuous and categorical variables. The continuous variables included; age, pulse at rest, systolic blood pressure (SBP) at rest, diastolic blood pressure (DBP) at rest, body weight, height, maximum heart rate (HR) on physical stress test, watt (WT) on physical stress test, metabolic equivalent (METs) on physical stress test, reached percent on physical stress test , ejection fraction (EF %) on echocardiography, estimated vessel age, right cardio-ankle vascular index (R-CAVI), left Cardio-ankle vascular index (L-CAVI), right ankle-brachial index (RABI), left ankle-brachial index (LABI), mean SBP brachial (SBPB) (=(right SBPB+ left SBPB)//2), mean DBPB (=(right DBPB + left DBPB)/2), BP right brachial (BPRB) (=(SBP+DBP)/2), BP left brachial (BPLB) (=(SBP+DBP)/2), mean BPB (=(BPRB+ BPLB)/2), BP right ankle (BPRA) (=(SBP+DBP)/2), BP left ankle (BPLA) (=(SBP+DBP)/2), mean BPA (=(BPRA+ BPLA) /2), mean ankle-brachial index (ABI), right brachial pulse (RTb), left brachial pulse (LTb), mean Tb (=(LTb+ RTb)/2), right brachial-ankle pulse (Tba), left brachial-ankle pulse (Tba), mean Tba (= (left Tba+right Tba)/2), length heart-ankle (Lha in cm), heart-ankle pulse wave velocity (haPWV; m/s), β-stiffness index from PWV, creatinine (μmol/L) , and eGFR (2021 CKD-EPI Creatinine). The categorical variables included; gender, obesity stage, smoking, concomitant disease, atherosclerosis of the coronary artery, hemodynamically significant (>60%), myocardial perfusion defect after stress ATP, myocardial perfusion defect before stress ATP, atherosclerosis in other arteries (Yes/No), brachiocephalic, hypertension (AH), stage AH, degree AH, risk of cardiovascular disease (CVD), stable coronary artery disease (SCAD), functional class (FC) by WT, FC by METs, reaction type to stress test(positive/negative), and reason of discontinuation of the stress test.

The study used the following SCECG parameters:

• QTc duration (Bazett's formula);

• amplitude parameters (JA is the amplitude at point J in microV, TA is the amplitude of the T-wave in microV, PAn is the amplitude of the negative P-wave in microV);

• indices of asymmetry SBeta, Beta (ratio of the maximum modulus of the derivative value at the leading front of the T-wave to the maximum modulus of the value at the trailing front of the T-wave);

• spectral integrals of energy of R and T waves: QRS11energy (leading front of R—1st derivative), QRS12energy (trailing front of R—1st derivative), QRS2energy (R-wave as a whole—2nd derivative), TE1 (T-wave as a whole) - (the integral is calculated as the sum of energies at all points of the corresponding region);

• spectral integral set by the frequency grid 2 to 4 Hz, 4 to 8 Hz (QRSE1, QRSE2);

• frequency of the maximum energy of the leading and trailing fronts of the R wave (RonsF, RoffsF);

• rhythm variability (SDNN);

• ECG time markers: PpeakN, Rpeak, Speak, Tpeak, Tons, Toffs.

ECG time intervals were calculated not from the beginning of the cardiac cycle, but from a point on the isoline, two-thirds of the duration of the mean R-R interval from the previous R-wave (so called—Calculated point). All parameters, except for the indicators of rhythm variability, were averaged taking into account the pulse rate. Rhythm variability indicators were evaluated by the program without averaging the values. Thus, the time parameters of the ECG took into account not only the morphology of the cardiac cycle, but also changes the heart rate. Considering that averaged values were taken into account, a longer recording provides the most accurate parameters. This includes markers of the beginning or the end of the wave (Pfi, QRSst, QRSfi), the shift of the negative or positive maximum value relative to the beginning of the averaged complex (PpeakN, Rpeak, Speak, Tpeak), as well as the maximum slope of the waves (Tons, Toffs). QRSfi is the time interval from the calculated point to the end of the QRS complex, expressed in ms. Tpeak is the time interval from the calculated point to the peak of the T wave. Toffs is the time interval from the calculated point to the point of maximum steepness of the descending knee of the T wave [28].

Taking into account that the position of the calculated point depends on the R-R interval, it is possible to minimize the effect of heart rate on the time parameters of the cardiac cycle. These time parameters take into account not only the morphology of the QRS complex or T-wave, but also the temporal features of the entire cardiac cycle.

After logistic regression analysis including more than 200 ECG parameter listed above, the artificial intelligence method was used to find combinations with the highest accuracy for IHD determination.

Criteria for the study participants

The inclusion criteria included;

1. Participants age ≥ 40 years.
2. Participants with intact mental and physical activity.
3. Written consent to participate in the study, take blood samples, and anonymously publish the results of the study.
4. The participants of the control group are individuals without coronary artery disease, confirmed by the absence of the myocardial perfusion defect on the adenosine triphosphate stress myocardial perfusion computed tomography ((by using contrast enhanced multi-slice spiral computed tomography (CE-MSCT) using adenosine triphosphate (ATP)), and confirmed by medical history, previous medical tests, and retrospective interview of participants.
5. The participants of the experimental group are individuals with coronary artery disease, confirmed by myocardial perfusion defect on the adenosine triphosphate stress myocardial perfusion computed tomography, and confirmed by medical history, previous medical tests, and retrospective interview of participants.

Exclusion criteria:

1. Poor single-channel ECG and pulse wave recording quality
2. Failure of the stress test for reasons unrelated to heart disease
3. Reluctance to continue participating in the study.

Non-inclusion criteria

1. Pregnancy.
2. Diabetes mellitus
3. Presence of signs of acute coronary syndrome (myocardial infarction in the last two days), history of myocardial infarction;
4. Active infectious and non-infectious inflammatory diseases in the exacerbation phase;
5. Respiratory diseases (bronchial asthma, chronic bronchitis, cystic fibrosis);
6. Acute thromboembolism of pulmonary artery branches;
7. Aortic dissection;
8. Critical heart defects;
9. Active oncopathology;

10. Decompensation phase of acute heart failure;
11. Neurological pathology (Parkinson's disease, multiple sclerosis, acute psychosis, Guillain-Barré syndrome);
12. Cardiac arrhythmias that do not allow exercise ECG testing (Wolff-Parkinson-White syndrome, Sick sinus syndrome, AV block of II-III-degree, persistent ventricular tachycardia);
13. Diseases of the musculoskeletal system that prevent passing a stress test (bicycle ergometry);
14. Allergic reaction to iodine and/or adenosine triphosphate.

Data collection

All participants at rest pass registration of S-ECG and pulse wave before (during 3 minutes) and just after (during 3 minutes) physical stress test (bicycle ergometry) using a portable single-channel recorder (CARDO-QVARK ; Russia, Moscow) [29]. The SCECG and pulse wave results interpreted using machine learning models developed by the Sechenov University team [29, 30].

Both groups pass a vessel stiffness test and pulse wave recording as well as vascular age by using Fukuda Denshi device (VaSera VS-1500; Japan). Cuffs placed to assess the vascular stiffness (CAVI parameter) and the vascular age as well as the ancle-brachial index. [31]

Subsequently, participants pass exercise bicycle ergometry test (SCHILLER CS200 device; Bruce protocol or modified Bruce protocol). According to the results metabolic equivalent; Mets-BT (BT), the angina functional class (FC) in participants with positive stress test results determined. During the bicycle ergometry, the participants monitored with 12-lead ECG and manual blood pressure measurement, 1 time each 2 minutes. The rest time ECG and blood pressure monitoring continue for at least five minutes after the end of the stress bicycle ergometry test.

The procedure discontinues if: an increase in systolic blood pressure ≥ 220 mmHg, horizontal or down sloping ST segment depression on the ECG ≥ 1 mm, typical heart pain during test, ventricular tachycardia or atrial fibrillation, or other significant heart rhythm disorders were found. Moreover, stop the procedure if the target heart rate (86% of the 220-age) is reached.

Before performing CTP, all the participants present results of the venous creatinine level, eGFR (estimated glomerular filtration rate) according to the 2021 CKD-EPI Creatinine > 30 ml/min/1,73 m2, according to the recommendation for using this formula by the National kidney foundation and the American Society of Nephrology [32–35].

The participants of both groups got catheterization in the basilar vein or the radial vein for injection of contrast and ATP to performed pharmacological stress test to the heart by increasing heart rate during the stressed myocardial perfusion computer tomography imaging. Computer tomography was performed on Canon scanner with 640 slice, 0,5 mm thickness of slice, with contrast (Omnipaque, 50 ml), injected two times: in rest to get images for myocardial perfusion before test, and in 20 mints just after ATP had been injected in dose according to body weight.

The results of the myocardial perfusion considered positive if there was a perfusion defect after stress test or worsen the already existing at the rest phase perfusion defect.

Statistical processing was carried out using the R programming language v4.2 and Python v.3.10 [^R] [36, 37]. Statistically significant values considered at $p<0.05$.

Statistical analysis

For quantitative parameters, the nature of the distribution (using the Shapiro-Wilk test), the mean, the standard deviation, the median, the interquartile, the 95% confidence interval, the minimum and maximum values were determined. For categorical and qualitative features, the proportion and absolute number of values were determined.

Comparative analysis for normally distributed quantitative traits was carried out on the basis of Welch's t-test (2 groups); for abnormally distributed quantitative traits, using the Mann-Whitney U-test (2 groups).

Comparative analysis of categorical and qualitative features was carried out using the Pearson X-square criterion, in case of its inapplicability, using the exact Fisher test.

For Single channel ECG values, pre-load values (prefixed with " $q0$_" were used, and deltas between immediately after exertion ($q1$) and after 2nd single channel ECG record, were calculated:

$$q0 = before$$
$$q1 = after\ 1$$

Calculation of deltas:

$$dltq_{01} = q1 - q0$$

Outcome and feature selection

In order to assess the impact of factors on outcomes due to the small number of observations, it was decided to abandon the classic univariate and subsequent stepwise or multivariate

regression analysis. The effect of exhaled air and CARDO-QVARK on the target variable was assessed using a mathematical modeling conveyor.

Due to the small number of observations, the so-called external cross-validation was used to assess the model's performance to select predictors. Selection was made among the predictor levels before the sample (CARDO-QVARK results), and then the delta for CARDO-QVARK results, as calculated above.

The data was randomly split with a mixing procedure into 3 parts. Each part became a validation array, and the remaining 2/3 became a training array. Thus, 3 different models were trained on each iteration, and none of the models were validated on the same data as they were trained.

This iteration was repeated 500 times with different options for splitting the data into 3 parts [38]. This approach allows us to draw indirect conclusions about the possibility of generalizing the results of model quality into larger samples.

The purpose of this method was to select the predictors with the highest normalized coefficients for each constructed model, which was a logistic regression with L1 regularization (Lasso regression). For each model that showed the quality of the AUC classifier above 0.75 in the validation part of the sample, the selected predictors and the corresponding coefficients were taken. For each predictor, the coefficients were taken modulo, then averaged, after which the 5 predictors with the highest coefficients were used for subsequent validation.

The validation process consisted of using only 5 selected predictors to build the model. In other respects, 3-fold cross-validation with data mixing with subsequent evaluation of the results of 3 classifiers was also used. This was possible because the hyperparameters of the classifiers were the same, and all 3 validation samples together gave all the data in the total sample.

Results

The characteristics of the sample described in the tables bellow. (*Table 1A-B*)

Table 1A: Categorical variables presented in absolute and relative values of the study for true incidence of the stated factor. Abbreviations: CPT; stress myocardial perfusion computer tomography imaging. X^2 test used as a comparative test. * Values statically significant difference. Abbreviations: METs; metabolic equivalent.

Index	Factor	Group 1 (n=19). Positive CTP	Group 2 (n=19). Negative	p

			CTP	
Gender	F	10 (52.6%)	7 (36.8%)	0.328
	M	9 (47.4%)	12 (63.2%)	
Obesity stage	1 degree	3 (15.8%)	3 (15.8%)	>0.999
	Normal	8 (42.1%)	9 (47.4%)	
	Overweight	8 (42.1%)	7 (36.8%)	
Atherosclerotic vascular (Namely)	Carotid	1 (9.1%)	0 (0.0%)	>0.999
	Carotid. Brachiocephalic bifurcation	10 (90.9%)	4 (100.0%)	
Stage of hypertension	I	2 (25.0%)	1 (7.1%)	0.179
	II	3 (37.5%)	11 (78.6%)	
	III	3 (37.5%)	2 (14.3%)	
Degree of hypertension	Degree 1	4 (50.0%)	7 (50.0%)	0.366
	Degree 2	1 (12.5%)	5 (35.7%)	
	Degree 3	3 (37.5%)	2 (14.3%)	
Risk of cardiovascular disease	High	3 (15.8%)	7 (36.8%)	0.486
	Low	7 (36.8%)	4 (21.1%)	
	Moderate	7 (36.8%)	7 (36.8%)	
	Very high	2 (10.5%)	1 (5.3%)	
Blood pressure reaction type on stress test	Asthenic	2 (10.5%)	1 (5.3%)	0.302
	Hypertonic	1 (5.3%)	1 (5.3%)	
	Hypotonic	3 (15.8%)	0 (0.0%)	

	Mild Hypertonic	1 (5.3%)	1 (5.3%)	
	Normotonic	12 (63.2%)	16 (84.2%)	
Watt	75	4 (21.1%)	7 (36.8%)	0.167
	100	8 (42.1%)	2 (10.5%)	
	125	4 (21.1%)	3 (15.8%)	
	150	1 (5.3%)	2 (10.5%)	
	175	0 (0.0%)	2 (10.5%)	
	200	1 (5.3%)	3 (15.8%)	
	250	1 (5.3%)	0 (0.0%)	
Functional class by Watt	FC-I	2 (40.0%)	3 (42.9%)	>0.999
	FC-II	3 (60.0%)	4 (57.1%)	
Functional class by METs	FC-I	1 (20.0%)	3 (42.9%)	0.735
	FC-II	4 (80.0%)	3 (42.9%)	
	FC-III	0 (0.0%)	1 (14.3%)	
Reaction type to stress test (positive/negative)	Negative	8 (42.1%)	9 (47.4%)	0.593
	Positive	5 (26.3%)	7 (36.8%)	
	Suspected	6 (31.6%)	3 (15.8%)	
Reason of discontinuation of the stress test	Horizontal ST depression >1mm	2 (10.5%)	4 (21.1%)	0.660
	Reach goal HR	17 (89.5%)	15 (78.9%)	
Tolerance to exertion on stress test	Close to high	2 (10.5%)	2 (10.5%)	0.830
	High	2 (10.5%)	2 (10.5%)	

	Low	0 (0.0%)	1 (5.3%)	
	Moderate	13 (68.4%)	10 (52.6%)	
	Very high	2 (10.5%)	4 (21.1%)	
Biological estimated vascular age	High	10 (52.6%)	9 (47.4%)	0.746
	Normal	9 (47.4%)	10 (52.6%)	
CKD stage	I	6 (31.6%)	10 (52.6%)	0.078
	II	9 (47.4%)	9 (47.4%)	
	IIIa	4 (21.1%)	0 (0.0%)	

Table 1B: The continuous variables of the sample presented as a mean ± standard deviation (Std. div.), Student test as independent variables used. * Values statically significant difference. Abbreviations: SBP; systolic blood pressure, DBP; diastolic blood pressure, BMI, body mass index, HR; heart rate, METs; metabolic equivalent, R-CAVI; right Cardio-ankle vascular index, L-CAVI; left Cardio-ankle vascular index, RABI; right ankle-brachial index, LABI; left ankle-brachial index, SBP B; systolic blood pressure brachial, DBP B; diastolic blood pressure brachial, BP RB; blood pressure right brachial, BP RA ; blood pressure right ankle, BP LA; blood pressure left ankle, BP A; blood pressure ankle, ABI; ankle-brachial index, RTb; right brachial pulse, LTb; left brachial pulse, Tb; mean brachial pulse, Tba; mean brachial-ankle pulse, Lha (cm); length heart-ankle, haPWV (m/s); heart-ankle pulse wave velocity.

Index	Group 1 (n=19). Positive CTP. Mean ± Std. div.	Group 2 (n=19). Negative CTP. Mean ± Std. div.	p
Age	56.9 ± 6.2	60.6 ± 12.1	0.238
Pulse rest	73.2 ± 9.6	71.3 ± 11.1	0.578
SBP rest	124.4 ± 9.4	120.6 ± 14.8	0.354
DBP rest	79.1 ± 11.1	76.6 ± 8.2	0.429
Body weight	77.8 ± 17.4	74.0 ± 10.6	0.4

			18
Height	173.2 ± 10.3	169.4 ± 8.9	0.240
BMI	25.8 ± 4.3	25.9 ± 4.1	0.939
Goal heart rate (HR)	163.1 ± 6.2	159.4 ± 12.1	0.238
Maximum HR	149.5 ± 11.2	146.7 ± 19.7	0.748
Reached % of the target HR on stress test	91.8 ± 8.2	92.6 ± 14.9	0.665
METs	6.7 ± 2.0	6.5 ± 2.1	0.715
Ejection fraction (%)	64.6 ± 4.1	65.3 ± 5.4	0.726
Biological estimated vessel age	58.1 ± 7.6	62.6 ± 13.9	0.222
R-CAVI	8.5 ± 0.8	9.1 ± 1.8	0.292
L-CAVI	8.5 ± 0.7	9.0 ± 1.7	0.231
RABI	1.2 ± 0.1	1.1 ± 0.1	0.181
LABI	1.2 ± 0.1	1.1 ± 0.1	0.082
Mean SBP B	130.1 ± 8.7	133.2 ± 16.2	0.465
Mean DBP B	82.9 ± 8.4	83.5 ± 9.0	0.817
BP RB (=(SBP+DBP)/2)	100.7 ± 10.0	102.8 ± 14.0	0.589
BP LB (=(SBP+DBP)/2)	101.8 ± 10.6	103.7 ± 12.7	0.631

Mean BP B= (BP RB+ BP LB)/2	101.3 ± 10.1	103.3 ± 13.2	0.603
BP RA (=(SBP+DBP)/2)	105.3 ± 10.7	108.3 ± 14.1	0.473
BP LA (=(SBP+DBP)/2)	106.6 ± 9.6	106.9 ± 11.1	0.926
Mean BP A= (BP RA + BP LA)/2	106.0 ± 9.6	107.6 ± 12.1	0.647
Mean ABI= (RABI+LABI)/2	1.2 ± 0.1	1.1 ± 0.1	0.101
RTb	79.4 ± 8.9	78.7 ± 11.5	0.839
LTb	73.3 ± 6.5	74.8 ± 10.7	0.599
Mean Tb =(RTb+ LTb)/2	76.3 ± 7.0	76.8 ± 10.8	0.888
Right Tba	88.5 ± 10.9	77.4 ± 22.1	0.125
Left Tba	87.7 ± 9.0	79.0 ± 20.8	0.144
Mean Tba =(Right Tba+ Left Tba)/2	88.1 ± 9.8	78.2 ± 21.3	0.129
Lha (cm)	150.8 ± 8.4	147.7 ± 7.2	0.240
haPWV (m/s)	0.9 ± 0.1	1.0 ± 0.2	0.234
β-stiffness index from PWV	3.0 ± 0.6	3.3 ± 1.2	0.686
Creatinine (µmol/L)	83.9 ± 11.9	86.4 ± 19.4	0.636
eGFR (2021 CKD-EPI Creatinine)	84.5 ± 13.7	79.6 ± 17.4	0.345

The diagnostic accuracy of the bicycle ergometry

We examined the diagnostic accuracy of a standard exercise test on a bicycle ergometer. In the ROC analysis, where the predictor was the result of a sample with the results of the physical exertion "Reaction_type" = 'Positive', and the target variable was Myocardial_perfusion_defect_after_stress_ATP, the following results were obtained. (*Table 2*)

Table 2: The quality of the bicycle ergometry appeared quite low in our cohort.

Chars	Point estimate	95%CI
AUC	0.553	[0.406 ; 0.695]
Sensitivity	0.263	[0.067 ; 0.474]
Specificity	0.632	[0.409 ; 0.833]
Negative predictive value	0.462	[0.269 ; 0.654]
Positive predictive value	0.417	[0.143 ; 0.714]

CARDO-QVARK Feature selection with cross-validation

After performing pipeline for feature selection using 500 iterations with 3-fold outer cross-validation , 87 best models were selected, showing AUC $\geq$ 0.9 for the test set. All models were aggregated with their respective absolute coefficients, and then the median estimate of the coefficients for each feature was calculated. Below are the selected 20 predictors (the final model included the first 5). (*Table 3*)

Table 3: The 20 most statically significant features according to the build model. Dltq_01 indicates the difference between the selected single channel ECG features immediately after the stress minus the selected features before the stress test.

	Feature	Lasso absolute coefficient
1.	**dltq_01_Pan...31**	0.589804
2.	**dltq_01_SA**	0.509832
3.	**dltq_01_JA**	0.37366
4.	**dltq_01_TE1**	0.270038
5.	**dltq_01_TpTe**	0.258854

6.	**dltq_01_HFNoise**	0.248446
7.	**dltq_01_PpeakN**	0.206324
8.	**dltq_01_QRS11energy**	0.190459
9.	**dltq_01_TA**	0.15963
10.	**dltq_01_Sbeta**	0.150864
11.	**dltq_01_TE3**	0.138504
12.	**dltq_01_Tenergy**	0.125174
13.	**dltq_01_TE4**	0.116375
14.	**dltq_01_Tpenergy**	0.106516
15.	**dltq_01_QTc**	0.102957
16.	**dltq_01_TE2**	0.102495
17.	**dltq_01_HFQRS**	0.090197
18.	**dltq_01_SDNN**	0.082806
19.	**dltq_01_QRSE1**	0.082143
20.	**dltq_01_QRSw**	0.063462

The model was then rebuilt as follows. The top 5 predictors from *Table 3* were with the most mathematically importance according to the built model taken and included in the new LASSO regression model.

Then the leave-one-out cross-validation procedure was performed, which allowed us to obtain approximate estimates of sensitivity, specificity, positive and negative prognostic value. At each iteration of leave-one-out cross-validation , the quantitative predictors were normalized.

The quality of the classification is shown in the table below. (*Table 4*)

Table 4:The quality of the single channel ECG in the diagnosis of ischemic heart disease using the CARDO-QVARK .

Chars	Point estimate	95%CI
AUC	0.684	[0.527 ; 0.817]
Sensitivity	0.737	[0.533 ; 0.929]
Specificity	0.632	[0.391 ; 0.833]
Negative	0.706	[0.47 ; 0.917]

predictive value		
Positive predictive value	0.667	[0.444 ; 0.857]

Confidence results are calculated using a bootstrap. Due to the small number of observations, the 95% CI is quite wide. Comparison with load results was carried out using the McNemar test [39]. (*Figure 1*)

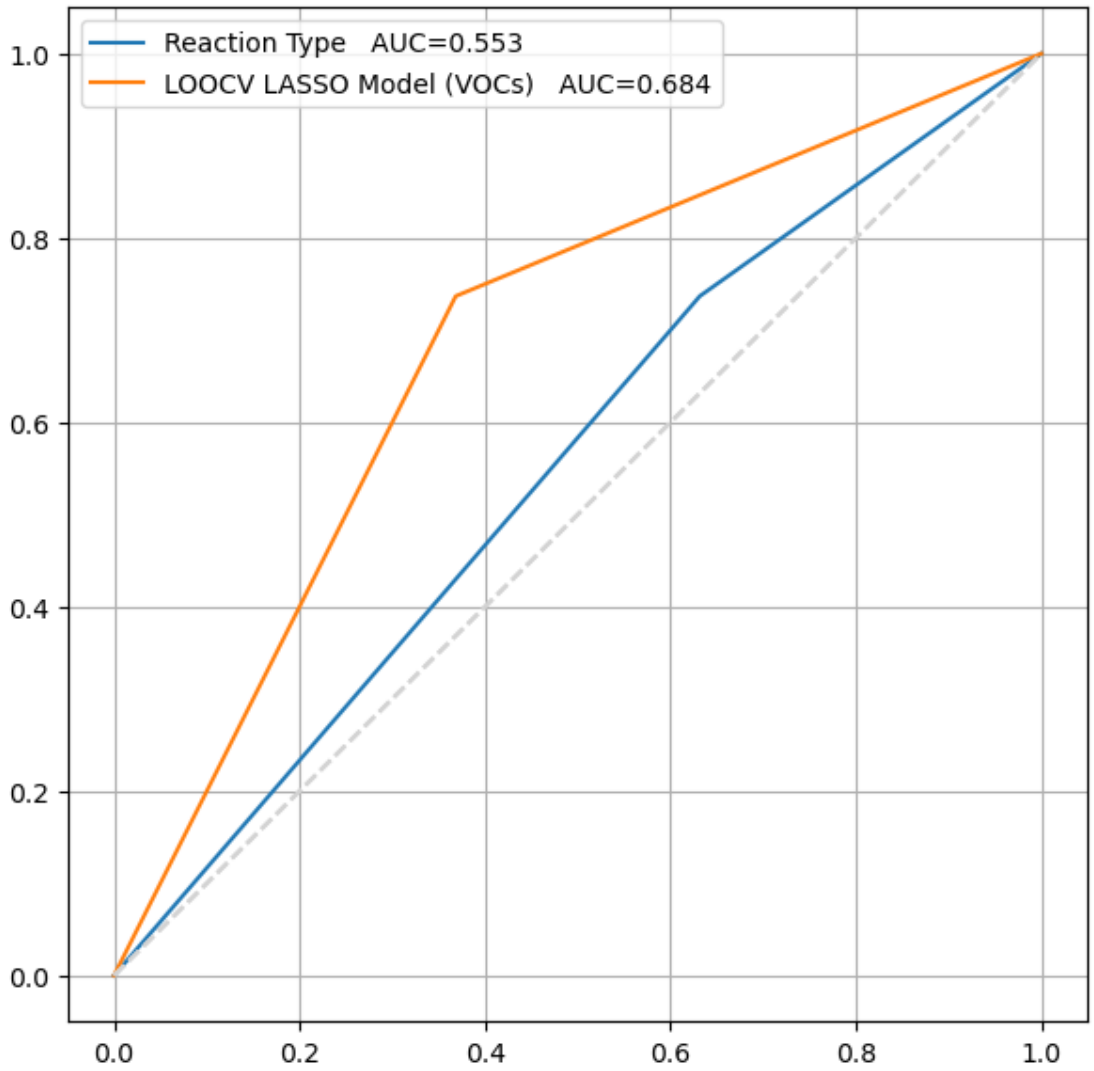

Figure 1: There is a significant difference between the results of the diagnostic accuracy of the load test (55.3 %) and the built model (68.4%), based on our study results. Obviously, the model has better predictive properties, P value = 0.0001.

The comparative statistical analysis demonstrated that the dltq_01_TpTe parameter has a statically significant difference between the two groups, in the first group, the mean ± Std. Div. 7.2 ± 28.1, and in the second group, the mean ± Std. Div. -12.2 ± 20.0, p value=0.046.

Discussion

Using single channel ECG in the diagnosis of ischemic heart disease is a potential novel diagnostic strategy. The usage of single channel ECG in optimizing the physical stress test such as bicycle ergometry [1]. Additionally, single channel ECG results can be interpreted using machine learning models to increase the diagnostic accuracy and used as a novel risk score for future cardiovascular events [10].

Several ongoing clinical trials to assess the reliability of single channel ECG in the diagnosis of ischemic heart disease and arrythmia in both adults and children (NCT05756309, NCT06181799).

Using physical stress tested monitored 12 lead-ECG remains the elementary test for the primary detection of ischemic heart disease. However, severe limitations exist in the diagnostic accuracy related to the ECG artifact during the movement of the patients during the physical stress test.

Improving the diagnostic accuracy of the physical stress test is a point of focus of the cardiological scientific community. Several attempts performed to enhance the diagnosis performance of the physical exertion tests using complementary methods such as the dynamics of cardiac electrical activity (EAS) during exercise testing [40]. The study suggests that incorporating the equivalent electric cardiac generator of dipole type during exercise ECG testing can enhance the accuracy of diagnosing coronary artery disease [40].

Previous clinical study using a Wearable wireless electrocardiographic (ECG) has shown that the single channel ECG has a poor sensitivity 8.3% (1.0–27.0%) and quite high specificity 89.9% (80.2–95.8%) for detection of reversible ischemic heart disease [41]. The study concluded that both 12-lead ECG (sensitivity 12.5% (3.0–34.4%), specificity 91.3% (82.0–96.7%)) and the single channel ECG have poor clinical usefulness in terms of ability to detect ischemic heart disease. Interestingly, a dramatic difference has been observed in the II lead of the 12- lead ECG in compare to the single channel ECG [41]. However, other studies suggested the use of deep learning models to enhance the diagnostic accuracy (sensitivity) of the ECG for ischemic heart disease in emergency department [42].

Advancements in single-channel ECG technology for the detection of ischemic heart disease demonstrated that machine learning models based on single-lead ECG and pulse wave parameters, along with age and gender, can simplify screening diagnostics of ejection fraction

decrease and diastolic dysfunction with high accuracy [37]. Furthermore, high-frequency ECG signals have shown increased sensitivity and early timing in diagnosing cardiac ischemia, and portable high-resolution ECG devices have demonstrated utility in acute emergency settings [43].

Conclusions

Single channel ECG (CARDO-QVARK) have a potential to be used as an additional method for the diagnosis of ischemic heart disease in combination with the physical stress test including bicycle ergometry. Further studies required on a larger sample size needed to confirm the usage of the CARDO-QVARK for the clinical use for the diagnosis of ischemic heart disease.

The following CARDO-QVARK parameter are of interest for further investigation to reveal the hidden diagnostic value in the diagnosis of ischemic heart disease, dltq_01_Pan...31, dltq_01_SA, dltq_01_JA, dltq_01_TE1, and dltq_01_TpTe. Further, study on a larger sample is ongoing on clinicaltrials.gov (NCT06181799).

List of abbreviations

CVD; cardiovascular disease, CTP; stress computed tomography myocardial perfusion imaging

Decelerations

1. Ethics approval and consent to participate: the study approved by the Sechenov University, Russia, from “Ethics Committee Requirement № 19-23 from 26.10.2023”. A written consent is taken from the study participants
2. Consent for publication: applicable on reasonable request
3. Availability of data and materials: applicable on reasonable request
4. Competing interests: The authors declare that they have no competing interests regarding publication.
5. Funding’s: The work financed by the Ministry of Science and Higher Education of the Russian Federation within the framework of state support for the creation and development of World-Class Research Center ‘Digital biodesign and personalized healthcare’ № 075-15-2022-304.
6. Authors' contributions: MB is the writer, researcher, collected and analyzed data, interpreted the results, and revised the final version of the manuscript, MA, collected part of the patients, AS analyzed the exhaled breath, AS biostatistical analysis of the sample, PCh, DG, NV, NM, AAB, SVK, EF, revised the paper, and PhK revised the final version of the manuscript. All authors have read and approved the manuscript.

7. Acknowledgments: not applicable

8. Authors' information: **Basheer Abdullah Marzoog**, World-Class Research Center «Digital Biodesign and Personalized Healthcare», I.M. Sechenov First Moscow State Medical University (Sechenov University), 119991 Moscow, Russia; postal address: Russia, Moscow, 8-2 Trubetskaya street, 119991. (marzug@mail.ru, +79969602820). ORCID: 0000-0001-5507-2413. Scopus ID: 57486338800. **Magomed Abdullaev**, World-Class Research Center «Digital Biodesign and Personalized Healthcare», I.M. Sechenov First Moscow State Medical University (Sechenov University), 119991 Moscow, Russia; postal address: Russia, Moscow, 8-2 Trubetskaya street, 119991. ORCID: 0000-0002-0451-2009. email: m.ba.m@icloud.com. **Peter Chomakhidze**, World-Class Research Center «Digital Biodesign and Personalized Healthcare», I.M. Sechenov First Moscow State Medical University (Sechenov University), 119991 Moscow, Russia; postal address: Russia, Moscow, 8-2 Trubetskaya street, 119991. ORCID: 0000-0003-1485-6072. email: m.ba.m@bk.ru. **Daria Gognieva**, World-Class Research Center «Digital Biodesign and Personalized Healthcare», I.M. Sechenov First Moscow State Medical University (Sechenov University), 119991 Moscow, Russia; postal address: Russia, Moscow, 8-2 Trubetskaya street, 119991. ORCID: 0000-0002-0451-2009. email: gognievad_g@staff.sechenov.ru. **Nina Vladimirovna Gagarina,** University clinical Hospital number 1, Radiology department, I.M. Sechenov First Moscow State Medical University (Sechenov University), 119991 Moscow, Russia; postal address: Russia, Moscow, 8-2 Trubetskaya street, 119991. Scopus ID: 6508312251. m.ba98@bk.ru. **Natalia Mozzhukhina,** University clinical Hospital number 1, Health Management Clinic, I.M. Sechenov First Moscow State Medical University (Sechenov University), 119991 Moscow, Russia; postal address: Russia, Moscow, 8-2 Trubetskaya street, 119991. ORCID: 0009-0002-7334-6945. v.t.i.m.b@outlook.com. **Sergey Vladimirovich Kostin,** National Research Ogarev Mordovia State University. Russia, Republic of Mordovia, Saransk, Bolshevistskaya str., 68, Saransk, Mordovia Republic, 430005. email: drmosalah@mail.ru. **Alexander Suvorov,** World-Class Research Center «Digital Biodesign and Personalized Healthcare», I.M. Sechenov First Moscow State Medical University (Sechenov University), 119991 Moscow, Russia; postal address: Russia, Moscow, 8-2 Trubetskaya street, 119991. email: suvorovayu1@staff.sechenov.ru. **Afina Aftandilovna Bestavashvili,** World-Class Research Center «Digital Biodesign and Personalized Healthcare», I.M. Sechenov First Moscow State Medical University (Sechenov

University), 119991 Moscow, Russia; postal address: Russia, Moscow, 8-2 Trubetskaya street, 119991. email: basheermarzoog1998@gmail.com. **Ekaterina Fominykha,** University clinical Hospital number 1, Radiology department, I.M. Sechenov First Moscow State Medical University (Sechenov University), 119991, Moscow, Russia; postal address: Russia, Moscow, 8-2 Trubetskaya street, 119991. ORCID: 0000-0003-0288-7656. Email: Fominykhev@staff.sechenov.ru. **Philipp Kopylov,** director of the institute of the Research Center «Digital Biodesign and Personalized Healthcare», I.M. Sechenov First Moscow State Medical University (Sechenov University), 119991 Moscow, Russia; postal address: Russia, Moscow, 8-2 Trubetskaya street, 119991. ORCID: 0000-0002-4535-8685. Scopus ID: 6507736224. email: kopylovf_yu@staff.sechenov.ru

9. The paper has not been submitted elsewhere

STANDARDS OF REPORTING

STROBE guideline has been followed.

References

[1] Marzoog, B. A. Breathomics Detect the Cardiovascular Disease: Delusion or Dilution of the Metabolomic Signature. *Curr. Cardiol. Rev.*, **2024**, *20* (4). https://doi.org/10.2174/011573403X283768240124065853.

[2] Abdou, A.; Krishnan, S. Horizons in Single-Lead ECG Analysis From Devices to Data. *Front. Signal Process.*, **2022**, *2*, 866047.

[3] Avram, R.; Ramsis, M.; Cristal, A. D.; Nathan, V.; Zhu, L.; Kim, J.; Kuang, J.; Gao, A.; Vittinghoff, E.; Rohdin-Bibby, L.; et al. Validation of an Algorithm for Continuous Monitoring of Atrial Fibrillation Using a Consumer Smartwatch. *Hear. Rhythm*, **2021**, *18* (9), 1482–1490. https://doi.org/10.1016/j.hrthm.2021.03.044.

[4] Perez, M. V.; Mahaffey, K. W.; Hedlin, H.; Rumsfeld, J. S.; Garcia, A.; Ferris, T.; Balasubramanian, V.; Russo, A. M.; Rajmane, A.; Cheung, L.; et al. Large-Scale Assessment of a Smartwatch to Identify Atrial Fibrillation. *N. Engl. J. Med.*, **2019**, *381* (20), 1909–1917. https://doi.org/10.1056/NEJMoa1901183.

[5] Tison, G. H.; Sanchez, J. M.; Ballinger, B.; Singh, A.; Olgin, J. E.; Pletcher, M. J.; Vittinghoff, E.; Lee, E. S.; Fan, S. M.; Gladstone, R. A.; et al. Passive Detection of Atrial Fibrillation Using a Commercially Available Smartwatch. *JAMA Cardiol.*, **2018**, *3* (5), 409–416. https://doi.org/10.1001/jamacardio.2018.0136.

[6] Inui, T.; Kohno, H.; Kawasaki, Y.; Matsuura, K.; Ueda, H.; Tamura, Y.; Watanabe, M.; Inage, Y.; Yakita, Y.; Wakabayashi, Y.; et al. Use of a Smart Watch for Early Detection of Paroxysmal Atrial Fibrillation: Validation Study. *JMIR Cardio*, **2020**, *4* (1). https://doi.org/10.2196/14857.

[7] Koshy, A. N.; Sajeev, J. K.; Nerlekar, N.; Brown, A. J.; Rajakariar, K.; Zureik, M.; Wong, M. C.; Roberts, L.; Street, M.; Cooke, J.; et al. Smart Watches for Heart Rate Assessment in Atrial Arrhythmias. *Int. J. Cardiol.*, **2018**, *266*, 124–127. https://doi.org/10.1016/J.IJCARD.2018.02.073.

[8] Nazarian, S.; Lam, K.; Darzi, A.; Ashrafian, H. Diagnostic Accuracy of Smartwatches for the Detection of Cardiac Arrhythmia: Systematic Review and Meta-Analysis. *J. Med. Internet Res.*, **2021**, *23* (8). https://doi.org/10.2196/28974.

[9] Fatimah, B.; Singh, P.; Singhal, A.; Pramanick, D.; Pranav, S.; Pachori, R. B. Efficient Detection of Myocardial Infarction from Single Lead ECG Signal. *Biomed. Signal Process. Control*, **2021**, *68*, 102678. https://doi.org/10.1016/J.BSPC.2021.102678.

[10] Issa, M. F.; Yousry, A.; Tuboly, G.; Juhasz, Z.; AbuEl-Atta, A. H.; Selim, M. M. Heartbeat Classification Based on Single Lead-II ECG Using Deep Learning. *Heliyon*, **2023**, *9* (7), e17974. https://doi.org/10.1016/j.heliyon.2023.e17974.

[11] Zhao, X.; Zhang, J.; Gong, Y.; Xu, L.; Liu, H.; Wei, S.; Wu, Y.; Cha, G.; Wei, H.; Mao, J.; et al. Reliable Detection of Myocardial Ischemia Using Machine Learning Based on Temporal-Spatial Characteristics of Electrocardiogram and Vectorcardiogram. *Front. Physiol.*, **2022**, *13*, 854191. https://doi.org/10.3389/FPHYS.2022.854191/BIBTEX.

[12] Smith, W. M.; Riddell, F.; Madon, M.; Gleva, M. J. Comparison of Diagnostic Value Using a Small, Single Channel, P-Wave Centric Sternal ECG Monitoring Patch with a Standard 3-Lead Holter System over 24 Hours. *Am. Heart J.*, **2017**, *185*, 67–73. https://doi.org/10.1016/J.AHJ.2016.11.006.

[13] Xintarakou, A.; Sousonis, V.; Asvestas, D.; Vardas, P. E.; Tzeis, S. Remote Cardiac Rhythm Monitoring in the Era of Smart Wearables: Present Assets and Future Perspectives. *Front. Cardiovasc. Med.*, **2022**, *9*, 853614. https://doi.org/10.3389/FCVM.2022.853614/BIBTEX.

[14] Krasteva, V.; Jekova, I.; Schmid, R. Perspectives of Human Verification via Binary QRS Template Matching of Single-Lead and 12-Lead Electrocardiogram. *PLoS One*, **2018**, *13* (5). https://doi.org/10.1371/JOURNAL.PONE.0197240.

[15] Attia, Z. I.; Harmon, D. M.; Dugan, J.; Manka, L.; Lopez-Jimenez, F.; Lerman, A.;

514 Siontis, K. C.; Noseworthy, P. A.; Yao, X.; Klavetter, E. W.; et al. Prospective
515 Evaluation of Smartwatch-Enabled Detection of Left Ventricular Dysfunction. *Nat.*
516 *Med.*, **2022**, *28* (12), 2497–2503. https://doi.org/10.1038/s41591-022-02053-1.
517 [16] Gu, H. Y.; Huang, J.; Liu, X.; Qiao, S. Q.; Cao, X. Effectiveness of Single-Lead ECG
518 Devices for Detecting Atrial Fibrillation: An Overview of Systematic Reviews.
519 *Worldviews on Evidence-Based Nursing*. John Wiley and Sons Inc 2023.
520 https://doi.org/10.1111/wvn.12667.
521 [17] Rajakariar, K.; Koshy, A. N.; Sajeev, J. K.; Nair, S.; Roberts, L.; Teh, A. W. Accuracy
522 of a Smartwatch Based Single-Lead Electrocardiogram Device in Detection of Atrial
523 Fibrillation. *Heart*, **2020**, *106* (9), 665–670. https://doi.org/10.1136/HEARTJNL-2019-
524 316004.
525 [18] Sološenko, A.; Petrenas, A.; Paliakaite, B.; Sörnmo, L.; Marozas, V. Detection of
526 Atrial Fibrillation Using a Wrist-Worn Device. *Physiol. Meas.*, **2019**, *40* (2).
527 https://doi.org/10.1088/1361-6579/AB029C.
528 [19] Fan, Y. Y.; Li, Y. G.; Li, J.; Cheng, W. K.; Shan, Z. L.; Wang, Y. T.; Guo, Y. T.
529 Diagnostic Performance of a Smart Device with Photoplethysmography Technology
530 for Atrial Fibrillation Detection: Pilot Study (Pre-Mafa II Registry). *JMIR mHealth*
531 *uHealth*, **2019**, *7* (3). https://doi.org/10.2196/11437.
532 [20] Bumgarner, J. M.; Lambert, C. T.; Hussein, A. A.; Cantillon, D. J.; Baranowski, B.;
533 Wolski, K.; Lindsay, B. D.; Wazni, O. M.; Tarakji, K. G. Smartwatch Algorithm for
534 Automated Detection of Atrial Fibrillation. *J. Am. Coll. Cardiol.*, **2018**, *71* (21), 2381–
535 2388. https://doi.org/10.1016/J.JACC.2018.03.003.
536 [21] Vardas, P.; Cowie, M.; Dagres, N.; Asvestas, D.; Tzeis, S.; Vardas, E. P.; Hindricks,
537 G.; Camm, J. The Electrocardiogram Endeavour: From the Holter Single-Lead
538 Recordings to Multilead Wearable Devices Supported by Computational Machine
539 Learning Algorithms. *Europace*, **2020**, *22* (1), 19–23.
540 https://doi.org/10.1093/EUROPACE/EUZ249.
541 [22] Bayoumy, K.; Gaber, M.; Elshafeey, A.; Mhaimeed, O.; Dineen, E. H.; Marvel, F. A.;
542 Martin, S. S.; Muse, E. D.; Turakhia, M. P.; Tarakji, K. G.; et al. Smart Wearable
543 Devices in Cardiovascular Care: Where We Are and How to Move Forward. *Nat. Rev.*
544 *Cardiol.*, **2021**, *18* (8), 581–599. https://doi.org/10.1038/S41569-021-00522-7.
545 [23] Nault, I.; André, P.; Plourde, B.; Leclerc, F.; Sarrazin, J. F.; Philippon, F.; O'Hara, G.;
546 Molin, F.; Steinberg, C.; Roy, K.; et al. Validation of a Novel Single Lead Ambulatory
547 ECG Monitor – Cardiostat^{TM} – Compared to a Standard ECG Holter Monitoring. *J.*

Electrocardiol., **2019**, *53*, 57–63. https://doi.org/10.1016/J.JELECTROCARD.2018.12.011.

[24] Limitations of the Conventional ECG: Utility of Other Techniques. In *Clinical Electrocardiography: A Textbook*; wiley, 2021; pp 552–570. https://doi.org/10.1002/9781119536475.ch25.

[25] Braun, T.; Spiliopoulos, S.; Veltman, C.; Hergesell, V.; Passow, A.; Tenderich, G.; Borggrefe, M.; Koerner, M. M. Detection of Myocardial Ischemia Due to Clinically Asymptomatic Coronary Artery Stenosis at Rest Using Supervised Artificial Intelligence-Enabled Vectorcardiography – A Five-Fold Cross Validation of Accuracy. *J. Electrocardiol.*, **2020**, *59*, 100–105. https://doi.org/10.1016/j.jelectrocard.2019.12.018.

[26] Beck, S.; Martínez Pereyra, V.; Seitz, A.; Bekeredjian, R.; Sechtem, U.; Ong, P. Detection of ECG alterations typical for myocardial ischemia: New methods 2021. *Internist*, **2021**. https://doi.org/10.1007/s00108-021-01037-6.

[27] Hilbel, T.; Frey, N. Review of Current ECG Consumer Electronics (Pros and Cons). *J. Electrocardiol.*, **2023**, *77*, 23–28. https://doi.org/10.1016/j.jelectrocard.2022.11.010.

[28] Kuznetsova, N.; Gubina, A.; Sagirova, Z.; Dhif, I.; Gognieva, D.; Melnichuk, A.; Orlov, O.; Syrkina, E.; Sedov, V.; Chomakhidze, P.; et al. Left Ventricular Diastolic Dysfunction Screening by a Smartphone-Case Based on Single Lead ECG. *Clin. Med. Insights Cardiol.*, **2022**, *16*. https://doi.org/10.1177/11795468221120088.

[29] Gognieva, D.; Vishnyakova, N.; Mitina, Y.; Chomakhidze, P.; Mesitskaya, D.; Kuznetsova, N.; Khiari, M.; Ryabykina, G.; Boytsov, S.; Syrkin, A.; et al. Remote Screening for Atrial Fibrillation by a Federal Cardiac Monitoring System in Primary Care Patients in Russia: Results from the Prospective Interventional Multicenter FECAS-AFS Study. *Glob. Heart*, **2022**, *17* (1). https://doi.org/10.5334/gh.1057.

[30] Sagirova, Z.; Kuznetsova, N.; Gogiberidze, N.; Gognieva, D.; Suvorov, A.; Chomakhidze, P.; Omboni, S.; Saner, H.; Kopylov, P. Cuffless Blood Pressure Measurement Using a Smartphone-Case Based ECG Monitor with Photoplethysmography in Hypertensive Patients. *Sensors*, **2021**, *21* (10), 3525. https://doi.org/10.3390/s21103525.

[31] Shirai, K.; Hiruta, N.; Song, M.; Kurosu, T.; Suzuki, J.; Tomaru, T.; Miyashita, Y.; Saiki, A.; Takahashi, M.; Suzuki, K.; et al. Cardio-Ankle Vascular Index (CAVI) as a Novel Indicator of Arterial Stiffness: Theory, Evidence and Perspectives. *J. Atheroscler. Thromb.*, **2011**, *18* (11), 924–938. https://doi.org/10.5551/jat.7716.

582 [32] Cockcroft, D. W.; Gault, M. H. Prediction of Creatinine Clearance from Serum
583 Creatinine. *Nephron*, **1976**, *16* (1), 31–41. https://doi.org/10.1159/000180580.
584 [33] Winter, M. A.; Guhr, K. N.; Berg, G. M. Impact of Various Body Weights and Serum
585 Creatinine Concentrations on the Bias and Accuracy of the Cockcroft-Gault Equation.
586 *Pharmacotherapy*, **2012**, *32* (7), 604–612. https://doi.org/10.1002/j.1875-
587 9114.2012.01098.x.
588 [34] Brown, D. L.; Masselink, A. J.; Lalla, C. D. Functional Range of Creatinine Clearance
589 for Renal Drug Dosing: A Practical Solution to the Controversy of Which Weight to
590 Use in the Cockcroft-Gault Equation. *Ann. Pharmacother.*, **2013**, *47* (7–8), 1039–
591 1044. https://doi.org/10.1345/aph.1S176.
592 [35] Delgado, C.; Baweja, M.; Crews, D. C.; Eneanya, N. D.; Gadegbeku, C. A.; Inker, L.
593 A.; Mendu, M. L.; Miller, W. G.; Moxey-Mims, M. M.; Roberts, G. V.; et al. A
594 Unifying Approach for GFR Estimation: Recommendations of the NKF-ASN Task
595 Force on Reassessing the Inclusion of Race in Diagnosing Kidney Disease. *Am. J.*
596 *Kidney Dis.*, **2022**, *79* (2), 268-288.e1. https://doi.org/10.1053/j.ajkd.2021.08.003.
597 [36] Sagirova, Z. N.; Kuznetsova, N. O.; Suvorov, A. Y.; Gognieva, D. G.; Kulikov, V. M.;
598 Chomakhidze, P. S.; Andreev, D. A.; Kopylov, P. Y. Assessment of Left Ventricular
599 Systolic Function Using a Single-Channel ECG Monitor with Photoplethysmography
600 Based on Machine Learning Models. *Kardiol. i serdechno-sosudistaya khirurgiya*,
601 **2023**, *16* (1), 46. https://doi.org/10.17116/kardio20231601146.
602 [37] Kuznetsova, N.; Sagirova, Z.; Suvorov, A.; Dhif, I.; Gognieva, D.; Afina, B.;
603 Poltavskaya, M.; Sedov, V.; Chomakhidze, P.; Kopylov, P. A Screening Method for
604 Predicting Left Ventricular Dysfunction Based on Spectral Analysis of a Single-
605 Channel Electrocardiogram Using Machine Learning Algorithms. *Biomed. Signal*
606 *Process. Control*, **2023**, *86*, 105219. https://doi.org/10.1016/j.bspc.2023.105219.
607 [38] Cawley, G. C.; Talbot, N. L. C. On Over-Fitting in Model Selection and Subsequent
608 Selection Bias in Performance Evaluation. *J. Mach. Learn. Res.*, **2010**, *11*, 2079–2107.
609 [39] Marius, O. U.; Happiness, O.-I. An Extended McNemar Test for Comparing
610 Correlated Proportion of Positive Responses. *Biometrics Biostat. Int. J.*, **2019**, *8* (4),
611 125–137. https://doi.org/10.15406/bbij.2019.08.00281.
612 [40] Kramm, M. N.; Strelkov, N. O.; Chomakhidze, P. S.; Kopylov, F. Y. Study of
613 Additional Diagnostic Signs of Myocardial Ischemia. *Kardiol. i serdechno-sosudistaya*
614 *khirurgiya*, **2016**, *9* (1), 52. https://doi.org/10.17116/kardio20169152-57.
615 [41] Fabricius Ekenberg, L.; Høfsten, D. E.; Rasmussen, S. M.; Mølgaard, J.; Hasbak, P.;

Sørensen, H. B. D.; Meyhoff, C. S.; Aasvang, E. K. Wireless Single-Lead versus Standard 12-Lead ECG, for ST-Segment Deviation during Adenosine Cardiac Stress Scintigraphy. *Sensors*, **2023**, *23* (6), 2962. https://doi.org/10.3390/s23062962.

[42] Lee, B. T.; Kwon, J.; Cho, J.; Bae, W.; Park, H.; Seo, W.-W.; Cho, I.; Lee, Y.; Park, J.; Oh, B.-H.; et al. Usefulness of Deep-Learning Algorithm for Detecting Acute Myocardial Infarction Using Electrocardiogram Alone in Patients With Chest Pain at Emergency Department: DAMI-ECG Study. *J. Cardiovasc. Interv.*, **2023**, *2* (2), 100. https://doi.org/10.54912/jci.2022.0028.

[43] Srinivasan, A.; Vijayalakshmi, K.; Padmanabhan, D.; Shanmugam, K. Early Detection of Ischaemia Through High Frequency ECGs: The Role of Medical-Grade Wearables for Chest Pain Triages. In *2022 IEEE International Conference on Electronics, Computing and Communication Technologies, CONECCT 2022*; Institute of Electrical and Electronics Engineers Inc.: B. M. S College of Engineering, Dept. of Ece, Karnataka, Bangalore, India, 2022. https://doi.org/10.1109/CONECCT55679.2022.9865756.

Figure legends

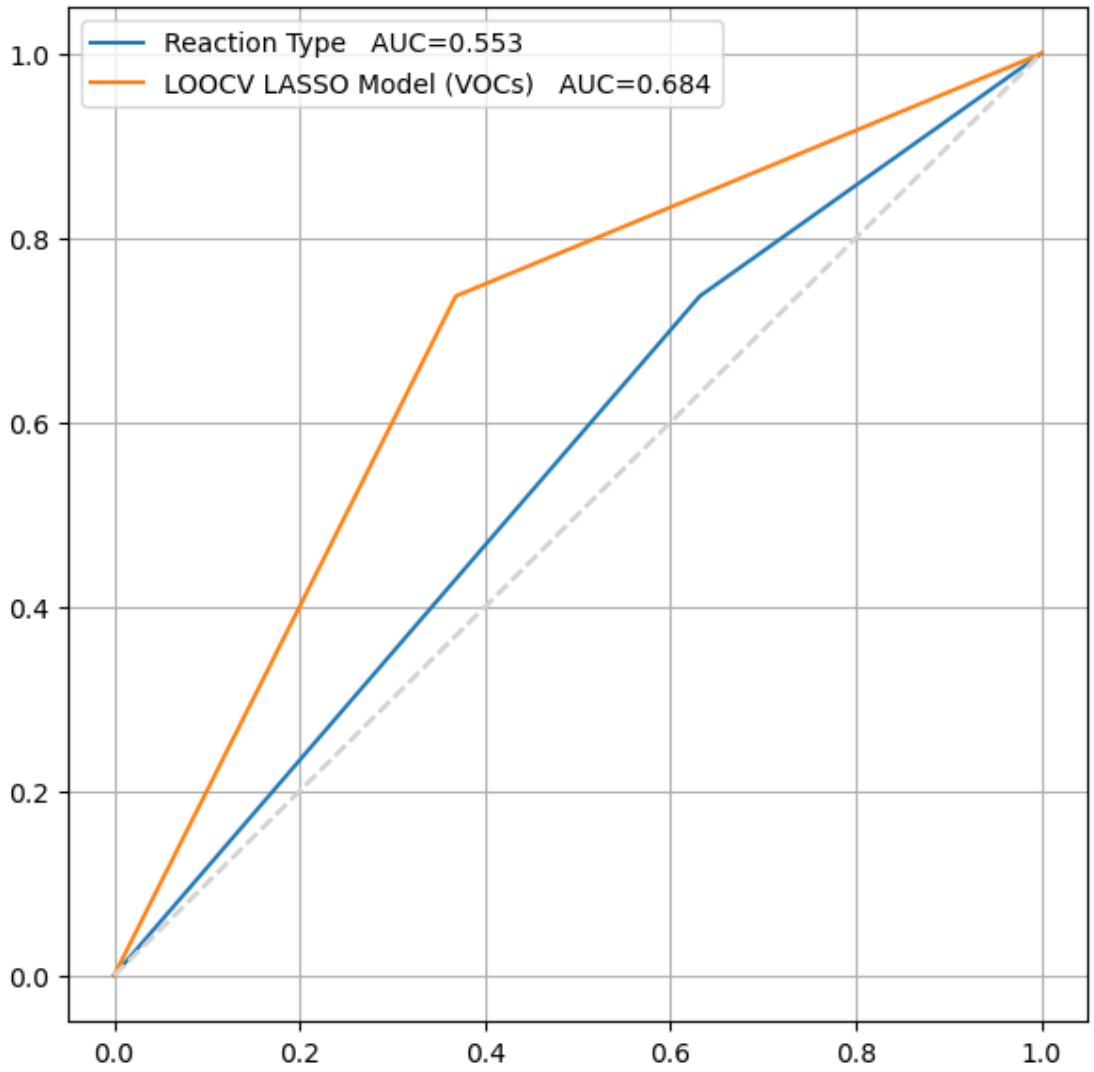

Figure 2: There is a significant difference between the results of the diagnostic accuracy of the load test (55.3 %) and the built model (68.4%), based on our study results. Obviously, the model has better predictive properties, P value = 0.0001.

Table legends

Table 5A: Categorical variables presented in absolute and relative values of the study for true incidence of the stated factor. Abbreviations: CPT; stress myocardial perfusion computer tomography imaging. X^2 test used as a comparative test. * Values statically significant difference. Abbreviations: METs; metabolic equivalent.

Index	Factor	Group 1 (n=19). Positive CTP	Group 2 (n=19). Negative CTP	p

Gender	F	10 (52.6%)	7 (36.8%)	0.328
	M	9 (47.4%)	12 (63.2%)	
Obesity stage	1 degree	3 (15.8%)	3 (15.8%)	>0.999
	Normal	8 (42.1%)	9 (47.4%)	
	Overweight	8 (42.1%)	7 (36.8%)	
Atherosclerotic vascular (Namely)	Carotid	1 (9.1%)	0 (0.0%)	>0.999
	Carotid. Brachiocephalic bifurcation	10 (90.9%)	4 (100.0%)	
Stage of hypertension	I	2 (25.0%)	1 (7.1%)	0.179
	II	3 (37.5%)	11 (78.6%)	
	III	3 (37.5%)	2 (14.3%)	
Degree of hypertension	Degree 1	4 (50.0%)	7 (50.0%)	0.366
	Degree 2	1 (12.5%)	5 (35.7%)	
	Degree 3	3 (37.5%)	2 (14.3%)	
Risk of cardiovascular disease	High	3 (15.8%)	7 (36.8%)	0.486
	Low	7 (36.8%)	4 (21.1%)	
	Moderate	7 (36.8%)	7 (36.8%)	
	Very high	2 (10.5%)	1 (5.3%)	
Blood pressure reaction type on stress test	Asthenic	2 (10.5%)	1 (5.3%)	0.302
	Hypertonic	1 (5.3%)	1 (5.3%)	
	Hypotonic	3 (15.8%)	0 (0.0%)	
	Mild	1 (5.3%)	1 (5.3%)	

	Hypertonic			
	Normotonic	12 (63.2%)	16 (84.2%)	
Watt	75	4 (21.1%)	7 (36.8%)	0.167
	100	8 (42.1%)	2 (10.5%)	
	125	4 (21.1%)	3 (15.8%)	
	150	1 (5.3%)	2 (10.5%)	
	175	0 (0.0%)	2 (10.5%)	
	200	1 (5.3%)	3 (15.8%)	
	250	1 (5.3%)	0 (0.0%)	
Functional class by Watt	FC-I	2 (40.0%)	3 (42.9%)	>0.999
	FC-II	3 (60.0%)	4 (57.1%)	
Functional class by METs	FC-I	1 (20.0%)	3 (42.9%)	0.735
	FC-II	4 (80.0%)	3 (42.9%)	
	FC-III	0 (0.0%)	1 (14.3%)	
Reaction type to stress test (positive/negative)	Negative	8 (42.1%)	9 (47.4%)	0.593
	Positive	5 (26.3%)	7 (36.8%)	
	Suspected	6 (31.6%)	3 (15.8%)	
Reason of discontinuation of the stress test	Horizontal ST depression >1mm	2 (10.5%)	4 (21.1%)	0.660
	Reach goal HR	17 (89.5%)	15 (78.9%)	
Tolerance to exertion on stress test	Close to high	2 (10.5%)	2 (10.5%)	0.830
	High	2 (10.5%)	2 (10.5%)	
	Low	0 (0.0%)	1 (5.3%)	

	Moderate	13 (68.4%)	10 (52.6%)	
	Very high	2 (10.5%)	4 (21.1%)	
Biological estimated vascular age	High	10 (52.6%)	9 (47.4%)	0.746
	Normal	9 (47.4%)	10 (52.6%)	
CKD stage	I	6 (31.6%)	10 (52.6%)	0.078
	II	9 (47.4%)	9 (47.4%)	
	IIIa	4 (21.1%)	0 (0.0%)	

Table 1B: The continuous variables of the sample presented as a mean ± standard deviation (Std. div.), Student test as independent variables used. * Values statically significant difference. Abbreviations: SBP; systolic blood pressure, DBP; diastolic blood pressure, BMI, body mass index, HR; heart rate, METs; metabolic equivalent, R-CAVI; right Cardio-ankle vascular index, L-CAVI; left Cardio-ankle vascular index, RABI; right ankle-brachial index, LABI; left ankle-brachial index, SBP B; systolic blood pressure brachial, DBP B; diastolic blood pressure brachial, BP RB; blood pressure right brachial, BP RA ; blood pressure right ankle, BP LA; blood pressure left ankle, BP A; blood pressure ankle, ABI; ankle-brachial index, RTb; right brachial pulse, LTb; left brachial pulse, Tb; mean brachial pulse, Tba; mean brachial-ankle pulse, Lha (cm); length heart-ankle, haPWV (m/s); heart-ankle pulse wave velocity.

Index	Group 1 (n=19). Positive CTP. Mean ± Std. div.	Group 2 (n=19). Negative CTP. Mean ± Std. div.	p
Age	56.9 ± 6.2	60.6 ± 12.1	0.238
Pulse rest	73.2 ± 9.6	71.3 ± 11.1	0.578
SBP rest	124.4 ± 9.4	120.6 ± 14.8	0.354
DBP rest	79.1 ± 11.1	76.6 ± 8.2	0.429
Body weight	77.8 ± 17.4	74.0 ± 10.6	0.418

Height	173.2 ± 10.3	169.4 ± 8.9	0.240
BMI	25.8 ± 4.3	25.9 ± 4.1	0.939
Goal heart rate (HR)	163.1 ± 6.2	159.4 ± 12.1	0.238
Maximum HR	149.5 ± 11.2	146.7 ± 19.7	0.748
Reached % of the target HR on stress test	91.8 ± 8.2	92.6 ± 14.9	0.665
METs	6.7 ± 2.0	6.5 ± 2.1	0.715
Ejection fraction (%)	64.6 ± 4.1	65.3 ± 5.4	0.726
Biological estimated vessel age	58.1 ± 7.6	62.6 ± 13.9	0.222
R-CAVI	8.5 ± 0.8	9.1 ± 1.8	0.292
L-CAVI	8.5 ± 0.7	9.0 ± 1.7	0.231
RABI	1.2 ± 0.1	1.1 ± 0.1	0.181
LABI	1.2 ± 0.1	1.1 ± 0.1	0.082
Mean SBP B	130.1 ± 8.7	133.2 ± 16.2	0.465
Mean DBP B	82.9 ± 8.4	83.5 ± 9.0	0.817
BP RB (=(SBP+DBP)/2)	100.7 ± 10.0	102.8 ± 14.0	0.589
BP LB (=(SBP+DBP)/2)	101.8 ± 10.6	103.7 ± 12.7	0.631
Mean BP B= (BP RB+	101.3 ± 10.1	103.3 ± 13.2	0.6

BP LB)/2			03
BP RA (=(SBP+DBP)/2)	105.3 ± 10.7	108.3 ± 14.1	0.473
BP LA (=(SBP+DBP)/2)	106.6 ± 9.6	106.9 ± 11.1	0.926
Mean BP A= (BP RA + BP LA)/2	106.0 ± 9.6	107.6 ± 12.1	0.647
Mean ABI= (RABI+LABI)/2	1.2 ± 0.1	1.1 ± 0.1	0.101
RTb	79.4 ± 8.9	78.7 ± 11.5	0.839
LTb	73.3 ± 6.5	74.8 ± 10.7	0.599
Mean Tb =(RTb+ LTb)/2	76.3 ± 7.0	76.8 ± 10.8	0.888
Right Tba	88.5 ± 10.9	77.4 ± 22.1	0.125
Left Tba	87.7 ± 9.0	79.0 ± 20.8	0.144
Mean Tba =(Right Tba+ Left Tba)/2	88.1 ± 9.8	78.2 ± 21.3	0.129
Lha (cm)	150.8 ± 8.4	147.7 ± 7.2	0.240
haPWV (m/s)	0.9 ± 0.1	1.0 ± 0.2	0.234
β-stiffness index from PWV	3.0 ± 0.6	3.3 ± 1.2	0.686
Creatinine (μmol/L)	83.9 ± 11.9	86.4 ± 19.4	0.636
eGFR (2021 CKD-EPI Creatinine)	84.5 ± 13.7	79.6 ± 17.4	0.345

654

655

Table 6: The quality of the bicycle ergometry appeared quite low in our cohort.

Chars	Point estimate	95%CI
AUC	0.553	[0.406 ; 0.695]
Sensitivity	0.263	[0.067 ; 0.474]
Specificity	0.632	[0.409 ; 0.833]
Negative predictive value	0.462	[0.269 ; 0.654]
Positive predictive value	0.417	[0.143 ; 0.714]

Table 7: The 20 most statically significant features according to the build model. Dltq_01 indicates the difference between the selected single channel ECG features immediately after the stress minus the selected features before the stress test.

	Feature	Lasso absolute coefficient
21.	**dltq_01_Pan...31**	0.589804
22.	**dltq_01_SA**	0.509832
23.	**dltq_01_JA**	0.37366
24.	**dltq_01_TE1**	0.270038
25.	**dltq_01_TpTe**	0.258854
26.	**dltq_01_HFNoise**	0.248446
27.	**dltq_01_PpeakN**	0.206324
28.	**dltq_01_QRS11energy**	0.190459
29.	**dltq_01_TA**	0.15963
30.	**dltq_01_Sbeta**	0.150864
31.	**dltq_01_TE3**	0.138504
32.	**dltq_01_Tenergy**	0.125174
33.	**dltq_01_TE4**	0.116375
34.	**dltq_01_Tpenergy**	0.106516
35.	**dltq_01_QTc**	0.102957
36.	**dltq_01_TE2**	0.102495

37.	**dltq_01_HFQRS**	0.090197
38.	**dltq_01_SDNN**	0.082806
39.	**dltq_01_QRSE1**	0.082143
40.	**dltq_01_QRSw**	0.063462

Table 8:The quality of the single channel ECG in the diagnosis of ischemic heart disease using the CARDO-QVARK .

Chars	Point estimate	95%CI
AUC	0.684	[0.527 ; 0.817]
Sensitivity	0.737	[0.533 ; 0.929]
Specificity	0.632	[0.391 ; 0.833]
Negative predictive value	0.706	[0.47 ; 0.917]
Positive predictive value	0.667	[0.444 ; 0.857]